JMEPEG (2019) 28:3211–3219
https://doi.org/10.1007/s11665-019-03914-6

1059-9495/$19.00

Manufacturing of a Metal Matrix Composite Coating on a Polymer Matrix Composite Through Cold Gas Dynamic Spray Technique

Alessia Serena Perna, Antonio Viscusi, Antonello Astarita, Luca Boccarusso, Luigi Carrino, Massimo Durante, and Raffaele Sansone

(Submitted September 11, 2018; in revised form November 22, 2018; published online February 12, 2019)

In this work, the manufacturing through cold gas dynamic spray (cold spray or CS) of metallic composite coatings of Al-Al_2O_3 on organic composite substrates with thermoplastic PLA matrix and hemp fibers was studied. Alumina powders, with a mean diameter of 50 µm, were used blended with aluminum powders in three different weight concentration percentages (0, 15, 20, and 45%) as feedstock material in order to highlight and discuss the variations of the coating surface properties depending on the alumina percentage. The coatings were produced by using a low-pressure cold spray equipment. A detailed experimental campaign, including microstructural observations and confocal microscopy, was carried out to study the structure of the coatings. Moreover, the tribological behavior of the coatings was studied through both scratch test and pin-on-disk test. The experiments showed that a small addition of alumina improves the compactness of the coating and its resistance to scratch and wear behavior.

Keywords alumina, aluminum powder, ceramics, cold spray, hemp, metal matrix composite, natural fiber composite

1. Introduction

In the recent years, more and more interest was directed to the tailoring of materials: aiming to save resources and optimize properties, the materials are engineered to better respond to the requests that arise during commissioning (Ref 1). In this context, the composite materials have emerged thanks to the possibility of totally varying their characteristics by suitably choosing fibers and matrices (Ref 2-4). A further opportunity is to give different properties to the substrate and bulk material: it may be important, for example, to provide scratch and wear resistance to the workpiece surface and to assign the mechanical properties to the innermost layer (Ref 5). A possibility that has not yet been thoroughly explored, having to face the difficulty of coating thermosensitive materials such as polymer matrix composites, is producing composite coatings on composite substrates (Ref 6).

In fact, conventional coating techniques, like plasma spraying or thermal spraying, are not suitable for temperature-sensitive materials, such as composite materials or plastics (Ref 7). For these reasons, further techniques involving temperatures well below the melting point of the material have been investigated, and in this scenario, cold gas dynamic spray technology (commonly referred as cold spray) has gained increasing interest in this research context. In cold spray, high-velocity micron-sized particles of a powder impact on a substrate, forming a thin metallic layer (Ref 8). This technology produces near-theoretical density, thick coatings that exhibit good fatigue performances, high conductivity, excellent corrosion behavior and higher hardness and UTS than the bulk material, due to the intrinsic characteristics of the process (Ref 9-11). Because the particles are heated in the gas stream only to a fraction of their melting temperature, the cold spray could be an effective technique to create coatings with materials sensitive to high temperatures. Upon impact with a target surface, conversion of kinetic energy to plastic deformation occurs, the solid particles deform and bond together, granting strong adhesion of the powders on the substrate (Ref 12). Acceleration of particles to high velocities is obtained via expansion of a pressurized gas through a converging-diverging DeLaval nozzle (Ref 13). In order to adhere on the substrate, the particles have to reach a critical value of impact kinetic energy that depends on the mechanical and thermal properties of the sprayed particles, on the carrier gas temperature (Ref 14) and on the distance of the nozzle from the substrate, that is called standoff distance (Ref 15). This technology has been thoroughly studied and applied for metal substrates (Ref 16-18), but much less has been said about the application on fiber-reinforced plastics (FRPs) materials (Ref 19, 20). However, the deposition of cold-sprayed coatings on composite material substrates can be a very useful method to overcome some of the composites weaknesses (Ref 21). For example, the presence of a metallic coating can vary their electrical and thermal conductivities and improve their wear and flame resistance, and in the same case, it can change the surface aesthetics

This article is an invited submission to JMEP selected from presentations at the International Symposium on Dynamic Response and Failure of Composite Materials (Draf2018) held June 12-15, 2018, on the Island of Ischia, Italy, and has been expanded from the original presentation.

Alessia Serena Perna, Antonio Viscusi, Antonello Astarita, Luca Boccarusso, Luigi Carrino, and **Massimo Durante**, Department of Chemical, Materials and Production Engineering, University of Naples "Federico II", P.le Tecchio 80, 80125 Naples, Italy; and **Raffaele Sansone**, Sophia High Tech s.r.l, Via Romani, 228, 80048 Sant'Anastasia, Naples, Italy. Contact e-mail: antonello.astarita@unina.it.

appearance. In particular, considering that in the last decade the interest of natural fiber composites (NFCs), or bio-composites, is grooving more and more, it is interesting to consider them as a possible substrate to coat in order to extend their application fields. (Ref 22). These materials are gaining an increasing interest in materials research field (Ref 23, 24), due to the necessity to attain sustainability standards and the growing environmental awareness (Ref 25). Indeed, if, the on one hand, the use of the bio-composite materials is associated with a lot of advantages, on the other hand, some of their applications are quite limited due to intrinsic disadvantages that characterize the NFCs such as their poor wear and flame resistance and in some cases their aesthetic appearance.

Therefore, to overcome these issues related to their superficial properties, the deposition of a metallic coating can give an important contribution.

Among various kinds of natural fibers used as reinforcement in NFCs, the hemp fibers are one of the most interesting ones, they have low density, low cost, high specific strength when compared to glass or aramid fibers, and their plant can easily be grown around the world and has the ability to extract heavy metals from the soil makes. It has been investigated that producing hemp-based natural fiber-reinforced thermoplastic mats yield an appreciable reduction in costs of about 20% and weight reduction of 23% compared with commercially available glass fiber-reinforced composites (Ref 26).

Regarding the matrix, both thermoplastic and thermoset polymers were widely used as matrices of NFCs, but with the aim to use the most environmental polymeric materials, the polylactic acid (PLA) is one of the best candidates (Ref 27). It is a synthetic polymer derived from natural monomers (Ref 28, 29, 23, 30). Therefore, on the basis of what above said, hemp-PLA composite was selected as substrate of this work. In previous papers of the authors, pure aluminum was deposited on the same substrates (Ref 31) and a slight percentage of alumina was added aiming to improve the buildup of the coating (Ref 32); in this work, alumina was homogeneously dispersed in the powder mix. In fact, the presence of hard particles can lift the deposition efficiency up to 20-30%, reduce the porosity of the coating (1-7%), and remove poorly bonded particles on the substrate and have a peening effect on the substrate (Ref 33). Those particles create micro-asperities that favor the adhesion of the subsequent particles, widening the contact area of the surface with the powders (Ref 34). Moreover, creating cold-sprayed coatings of ductile metals mixed with brittle ceramic materials would enable physical and mechanical properties to be tailored. However, particles have to be plastically deformed in order to adhere to the coating and so less deformable materials, like ceramic, cannot be efficiently deposited for the lack of plastic deformation. Although they cannot produce a coating on their own, hard ceramic particles can remove contamination, oxides, and impurities on the surface and clean obstruction in the nozzle. The aim of this work is to investigate the adhesion mechanisms between the particles and the composite substrate and to highlight the influence of the coating composition, in terms of alumina quantity, on the surface proprieties of the polymer matrix substrate. Four different alumina/aluminum powder mixtures were investigated: 0, 15, 30, and 45% Al_2O_3 wt.%. In order to analyze the bonding between the coating and the substrate, the specimens were observed by scanning electron microscope (SEM), and tribological analyses (pin-on-disk test for the wear behavior, scratch test, and roughness measurements) were carried out in order to characterize the coating.

2. Materials and Methods

2.1 Manufacturing of the Composite Laminates

Hemp-PLA laminates were used as the substrate. The polymeric matrix chosen is made of films of biodegradable polylactic acid (4042D supplied by NatureWorks), while the reinforcement consists of a bidirectional woven hemp fabric, with an areal density equal to 160 g/m^2 (supplied by MAEKO S.r.l). The abovementioned woven hemp fabric used for the process was preliminarily treated by soaking it in 2% NaOH solution at room temperature for 30 min. After the treatment, fibers were scrupulously washed with water to remove any traces of alkali on the surface of the fiber and subsequently neutralized with 1% acetic acid solution and then dried in an oven 12 h at 60 °C.

Laminates with a mean thickness of 2.0 mm were manufactured through the compression molding technique under a pressure of 1.1 MPa applied for 5 min. The temperature was set to 170 °C, according to the melting temperature point of the polymer (Ref 35).

The mold was cooled down in air, while the pressure was kept constant.

The fiber volume fraction was set equal to 30% according to the literature (Ref 36-38) highlighting that this fiber content allows reaching the best quasi-static and dynamic mechanical properties.

In order to observe the cross section, the specimens were cut by means of a precision hacksaw and incorporated in thermoplastic resin (Lucite provided by Leco) (Ref 39).

2.2 Cold Spray Deposition Process

For the cold spray deposition, a Dymet 423 low-pressure cold spray machine was used and argon was adopted as carrier gas. The choice of low-pressure equipment is a consequence of the low velocities required when spraying on polymeric substrates (Ref 40).

Micron-sized powders of aluminum alloy Al-Si12 were used for the spraying process due to their high ductility and different percentage of alumina (Al_2O_3) that were mixed in, in order to investigate the influence of the metal matrix composite coatings on bio-composites surface properties. A micrograph of the powder mixture is shown in Fig. 1.

Aluminum and alumina powders are easily distinguishable as the former have a rounded morphology, due to their ductile nature, while the latter are clearly sharper and jagged. What was acknowledged by visual inspection was confirmed through an EDS (energy-dispersive x-ray spectrometry) analysis, whose results are shown in Fig. 2, highlighting that the aluminum/oxygen ratio is the one that characterizes alumina (37% Al, 63% O_2), and Fig. 3 where the composition shown is mostly aluminum (89% Al, 10%O_2). Carbon is present in the EDS spectrum as it is a coating element.

As for the particle size, the aluminum has a broad distribution, shown in Fig. 4, in order to promote a higher compaction factor among the particles of the coating. Alumina, instead, has a mean size of 50 μm, as noticeable in Fig. 5. As stated in Introduction, four different alumina/aluminum powder

mixtures were deposited: 0, 15, 30, and 45% Al_2O_3 wt.%. The values were chosen according to the literature. A minimum value of 15 wt.% of alumina particles was chosen as only approximately a 5% of the total amount of the ceramic powder used effectively embeds the coating. An alumina percentage of 45% should be considered as an upper limit value, as exceeding this quantity would cause the powder to erode and leave the coating (Ref 32). The powders were combined using a sound-assisted apparatus consisting of a Plexiglas fluidization column, complying with the process outlined in literature (Ref 41). The proper cold spray deposition parameters such as the inlet gas temperature, the inlet gas pressure, and the standoff distance were chosen according to the authors' previous work (Ref 31): those parameters are in the middle of the deposition feasibility window and were left unchanged, despite the use of different

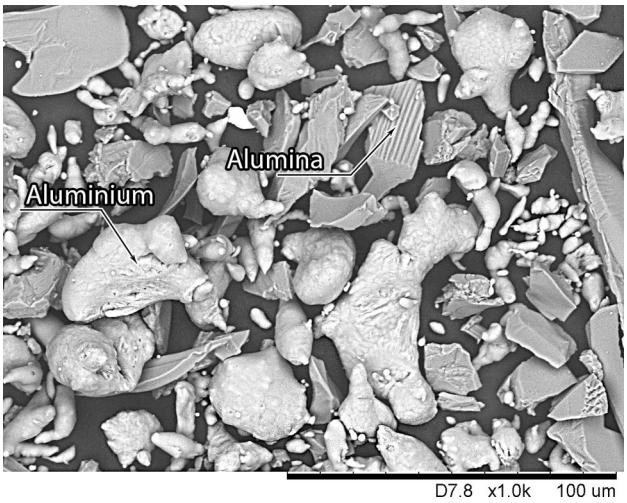

Fig. 1 SEM micrography of aluminum-alumina powder mixture

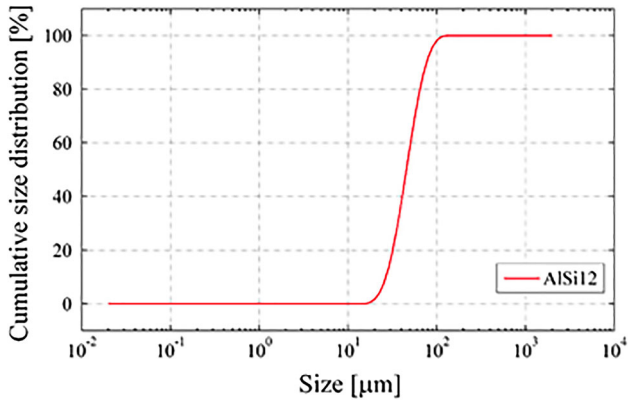

Fig. 4 Aluminum powder size distribution

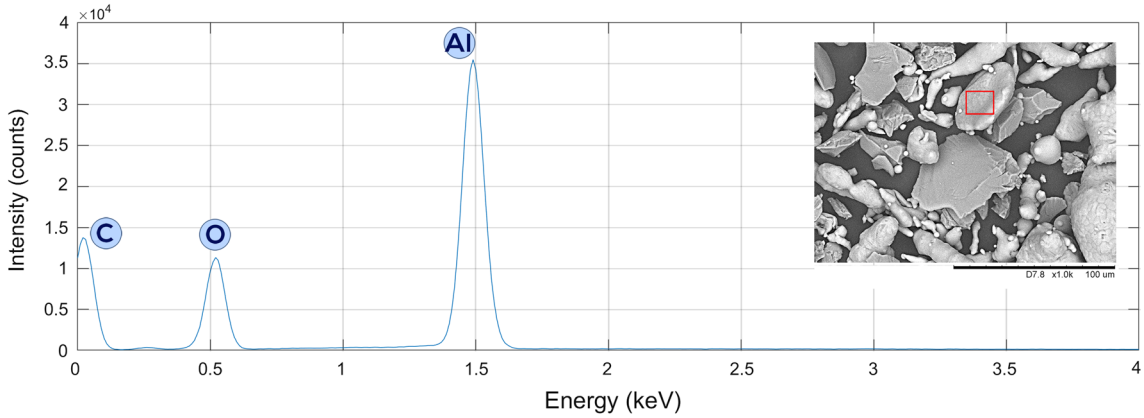

Fig. 2 Alumina EDS analysis results: the diagram portrays the mean values calculated on the surface delimited by the red square shown in the micrograph

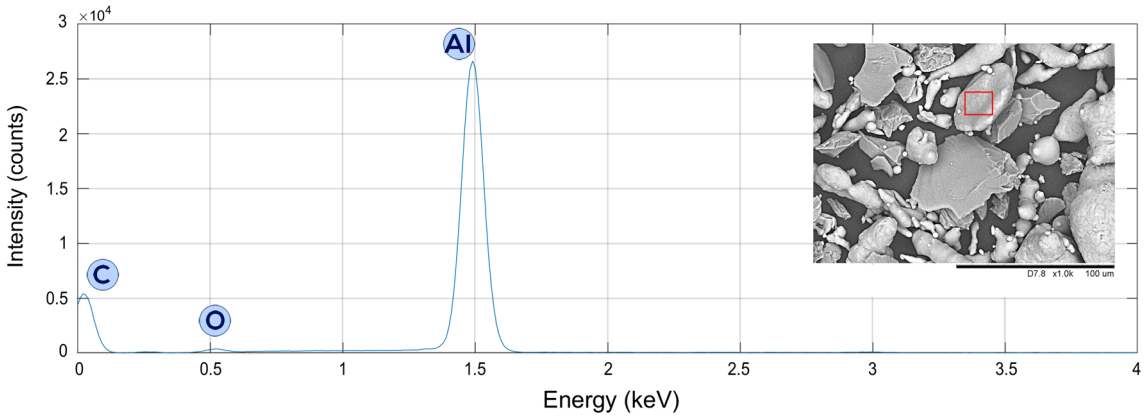

Fig. 3 Aluminum EDS analysis results: the diagram portrays the mean values calculated on the surface delimited by the red square shown in the micrograph

powders, in order to analyze only the influence of alumina. Coating tracks were produced with gas pressure of 7 bar and gas temperature set to 100 °C. The standoff distance remained fixed during the process and set to 50 mm. The process parameters were chosen by considering the necessity to accelerate the particles up to the required velocity to obtain adhesion and, in the same time, not heating up too much the substrate avoiding any damage within the panel. In fact, the problem of convective heat transfer, which can be neglected when the substrate is a metal, must be carefully considered when spraying on composite panels. The necessity to accelerate the particles arises because, in order to have effective deposition, the particle momentum has to be high enough to avoid the rebound of the particles while not reaching values that would cause strong erosion of the substrate or break the fibers, as stated in the literature (Ref 42, 43). A *k*-type thermocouple was used to measure the temperature of both the carrier gas at the exit section of the nozzle and the substrate during the whole process to set the process parameters properly. For each different powder mixture, a track 80 mm long and 40 mm wide was deposited with a single pass on the polymeric substrate with a travel speed of the spraying gun of 3 mm/s.

2.3 Characterization of the Coating

Several tribological and optical analyses were carried out in order to characterize the coating.

To observe the interface area between substrate and coating, SEM observations were performed by using a Hitachi TM 3000 SEM on the cross section of the specimens.

Roughness measurements were taken by means of a confocal microscope (Leica DCM3D). In this analysis, three roughness parameters, according to EN ISO 4287-1997 standard, were considered:

Ra, the most acknowledged parameter for evaluation of roughness, defined as the arithmetic mean of the absolute value of the height within a sampling area;
Rq, the root-mean-square value of ordinate values along the sampling length;
Rz, the maximum height of the roughness profile.

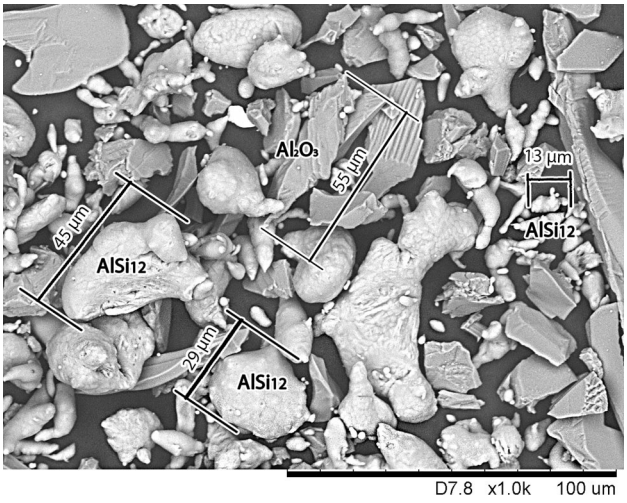

Fig. 5 Aluminum and alumina powder size examples

Pin-on-disk and scratch tests were also performed in order to characterize in a more complete way the coating proprieties: although panels are not usually subjected to slip and wear stresses, our goal is to analyze the overall behavior of the coating in order to leave open the possibility of different applications. As regards the pin-on-disk tests, it was carried out using a Ducom TR20-LE apparatus. The test consists of a fixed steel ball (8 mm in diameter) pressing against a rotating specimen under a fixed normal load of 5 N tracking circular tracks with a radius of 20 mm and constant peripheral speed of 209,4 mm/s for 96 min without lubricant. The results are provided in terms of depth of the track left by the passage of the pin. These results were followed by a confocal microscope analysis, which allowed to verify the depth values of the tracks and by optical microscope observations, for measuring the width of the tracks. The optical microscope used for this analysis was an Hirox KH8700.

During the scratch test, the diamond scratch tool, used for testing hard materials, is pressed against the surface of the specimen using a fixed load and then moved with a constant speed of 10,4 mm/s for fixed time steps (of 30, 60, and 90 s) along a 250-mm track. The aforementioned test was carried by means of Taber test machine. Both the tests were performed according, respectively, to ASTM G99, for the pin-on-disk test, and UNI EN 1071-3:2005 for the scratch test.

3. Results

3.1 Study of the Feasibility of the Deposition

The temperature measurements revealed that the highest temperature measured at the exit of the nozzle was 160 °C, while the substrate reached a maximum temperature of 120 °C, well below the melting point of the matrix (Ref 44), ensuring that its properties are not compromised.

From the visual inspection, it is immediately evident that there has been deposition of powders on the substrate, as shown in Fig. 6. The investigations carried out subsequently confirmed the effectiveness of this deposition.

The SEM analysis confirmed the correct adhesion: as shown in Fig. 7, the coating has penetrated the substrate more than 10 µm approximately, regardless of powder composition investigated. Moreover, as the alumina percentage in the powders

Fig. 6 Coating obtained through cold spray deposition. The sample depicted is the coating with 45% Al_2O_3 content

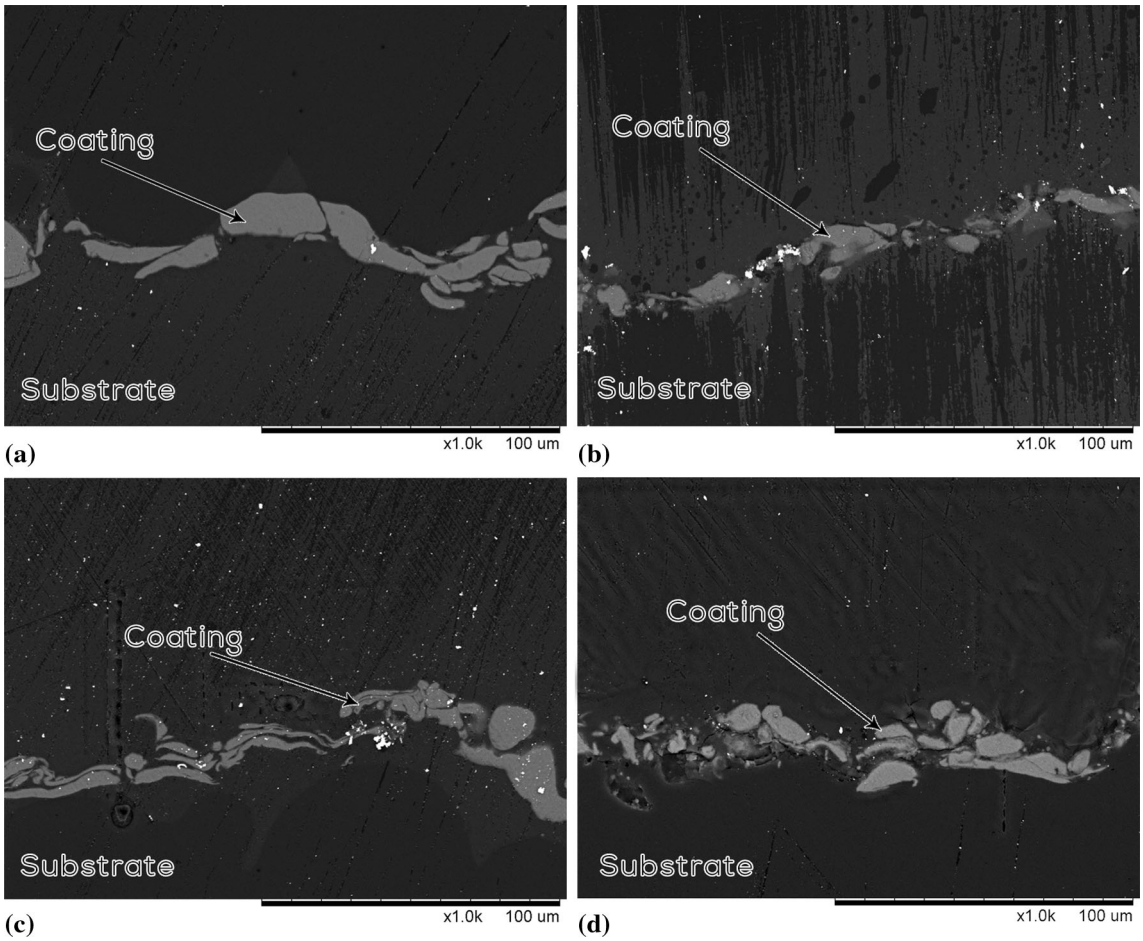

Fig. 7 SEM images of coatings with 0% (a), 15% (b), 30% (c), and 45% (d) Al_2O_3 content

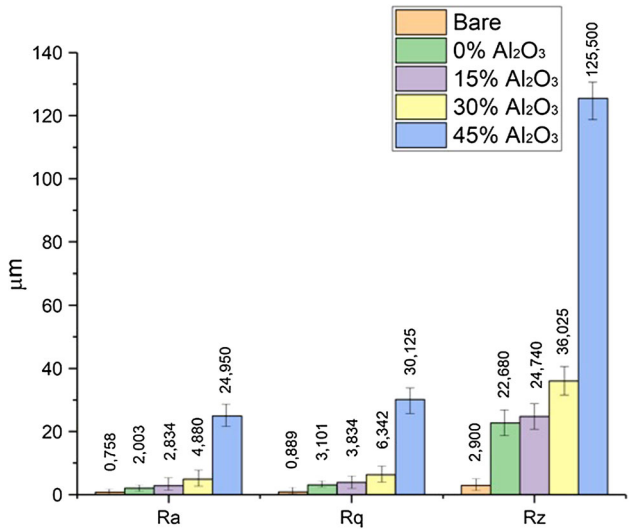

Fig. 8 Results and comparison of roughness analysis

increases, the harder particles have an intense peening effect (Ref 45, 46) and the coating tends to get denser. The values of surface roughness parameters for each kind of sample, obtained by using the confocal microscope, are shown in Fig. 8.

It seems evident that the roughness of the coatings has always a greater value than the roughness of the substrate, and this aspect can be explained due to the different nature of the compared surfaces.

In fact, from the comparison of the roughness values of the various coatings, it is clear that as the percentage of alumina present in the mixture of powders increases, the roughness increases.

In particular, the coating made with a mixture of powders containing 45% of alumina appears to have a roughness significantly higher than all the others; in fact, with reference to the average roughness value Ra, there is an increase of 500% in passing from the coating containing 30% of alumina to that with 45%. This can be explained as the process parameters chosen were same in each deposition, proving to be inadequately low for mixtures of powders with such a high content of Al_2O_3 particles. Moreover, alumina particles deform their shape less than aluminum particles during the impact. It should be noticed that a higher roughness is preferred when it is intended to carry out painting operations as it increases the adhesion of the paint (Ref 47). Furthermore, alumina hard ceramic powders produce micro-asperities that promote the bonding of the subsequent Al particles that impact on the coating underneath and widen the contact area between the substrate and the coating. However, another phenomenon emerges when the percentage of alumina is high, nullifying the beneficial effect on the growth of the coating: the alumina particles impact with high kinetic energy on the lower layers. Since a lower amount of energy is dissipated due to the

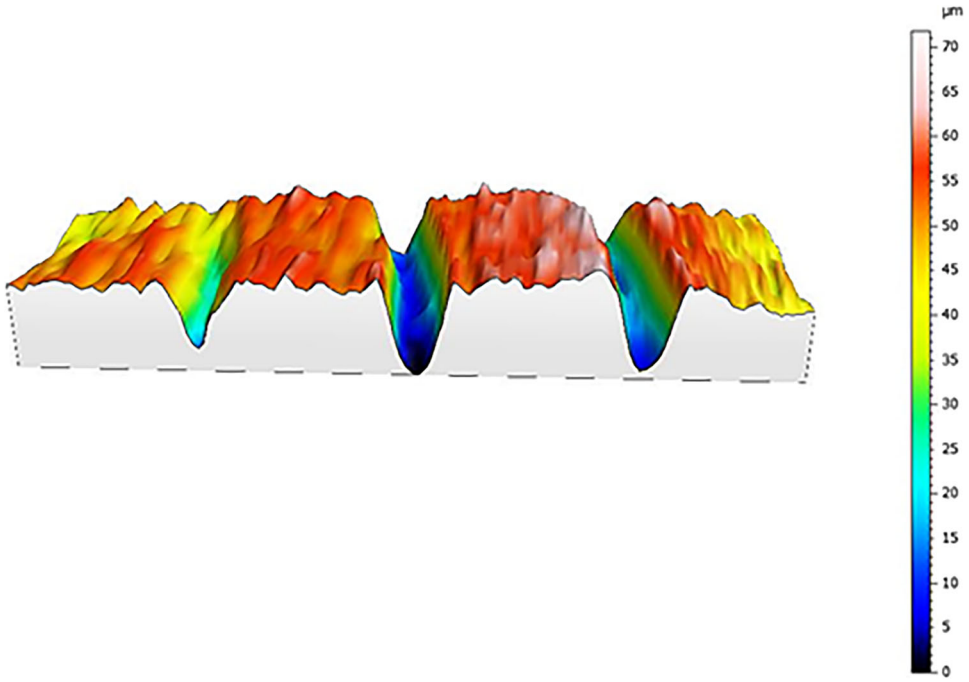

Fig. 9 Confocal image of the 15% Al_2O_3 specimen for evaluation of the depth of the tracks on the coating after the pin-on-disk test

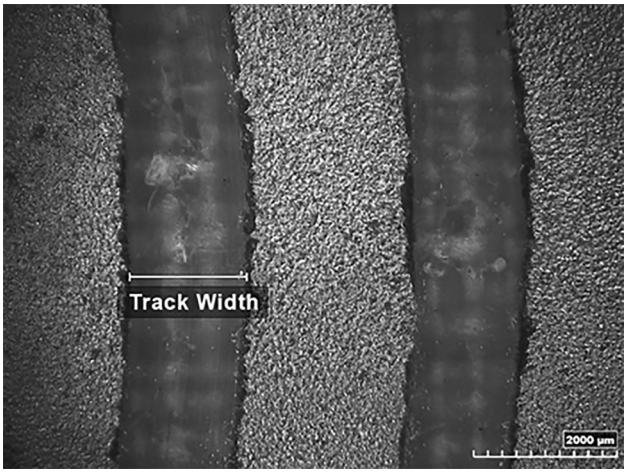

Fig. 10 Hirox image of the 0% Al_2O_3 specimen for evaluation of the width of the tracks on the coating after the pin-on-disk test

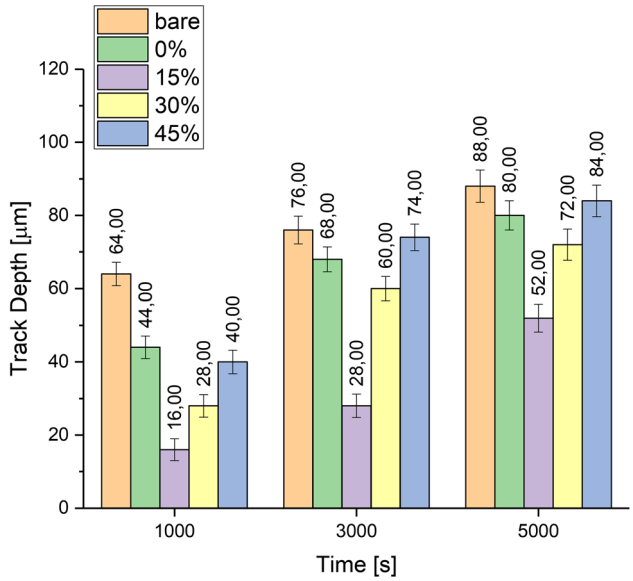

Fig. 11 Results and comparison of pin-on-disk test in terms of depth of the tracks [µm]

deformation, we would, therefore, have that the particles with high energy, impacting the newly formed coating, tear off a part of it preventing further growth. When alumina percentage reaches the 45%, this phenomenon prevails on the positive effect on bonding carried out by alumina particles, resulting in a discontinuous thin coating (Ref 32, 48).

Example images of the confocal microscope acquisition and Hirox micrography used to evaluate the track's parameters are shown in Fig. 9 and 10, respectively.

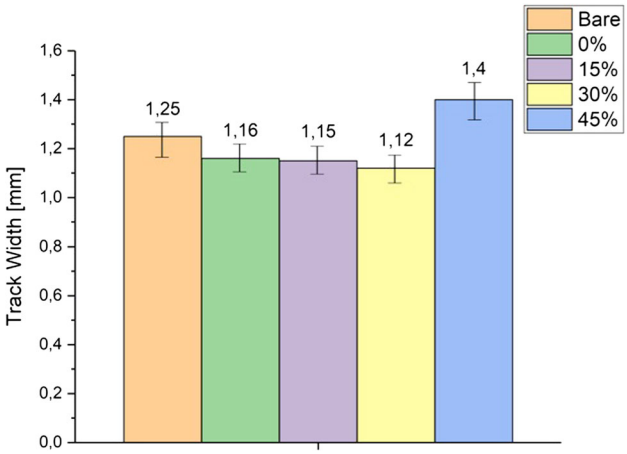

Fig. 12 Results and comparison of pin-on-disk test in terms of the width of the tracks [mm]

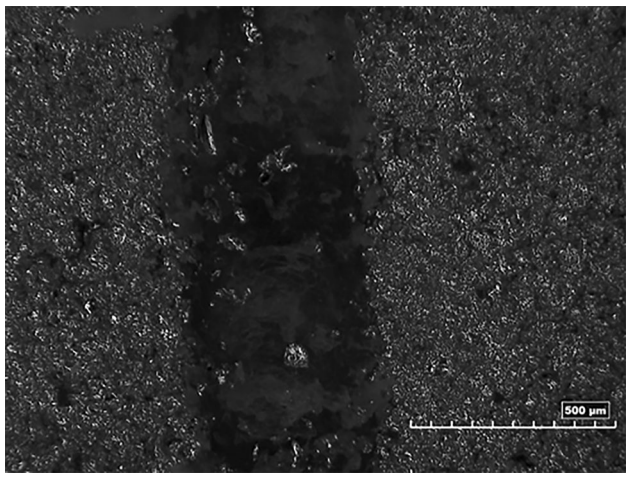

Fig. 14 Hirox image for evaluation of the width of the tracks on the coating after the scratch test

By looking at Fig. 11, it can be seen that with the increase in alumina concentration, the tribological performance of the composite systems initially tends to increase, as the pin penetrates less in the coating. However, when the concentration exceeds the 15%, the behavior of the coating tends to get worse due to the loads applied; therefore, alumina starts to break away from the coating causing an overall worsening of the proprieties. Analyzing these results, two main phenomena emerged: adding a small percentage of alumina increases the compaction factor and hardens the coating; this results in better wear and hardness proprieties.

It is noticeable that for a 45% of alumina, the wear behavior seems to be worse than the uncoated substrate also in terms of width of the trail, as shown in Fig. 12: with such a high concentration of alumina, powders start to migrate from the coating acting as abrasive particles and worsening the results. It also has to be noticed that the width of the track may increases due to the erosion of the pin as we can clearly see in Fig. 13: Alumina particles tend to consume the pin more than pure aluminum causing an overall widening of the track as the contact surface gets broader.

As for the scratches test, the depth and width measures of the scratches made on the various coatings were estimated with observations under the Hirox microscope: in Fig. 14, we can see the track left from the penetrator during the abovementioned test.

The diagrams shown in Fig. 15 and 16 report the results of the scratch test; each figure highlights the behavior of the different coatings, fixing the applied load, as the duration of the tests varies.

As can clearly seen in the previous figures, the depth and width of the track left from the scratch tools decrease as alumina is added to the coating, but just like it was noticed with pin-on-disk test, a worse behavior occurs when the quantity of Al_2O_3 exceeds the 30%.

By looking at these figures, another phenomenon emerges in this case: when the percentage of alumina is over 30%, alumina particle migrates from the coating to the diamond tool, acting as a built-up edge.

(a) **(b)**

Fig. 13 Pin surface erosion after the test (3000 s): a) pin used to test a 45% Al_2O_3 specimen and b) pin used to test a 15% Al_2O_3 specimen

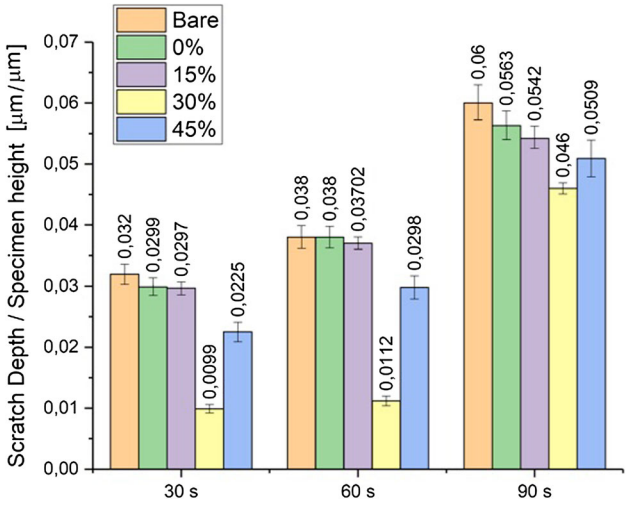

Fig. 15 Results and comparison of scratch test in terms of depth of the tracks, normalized on the total height [mm]

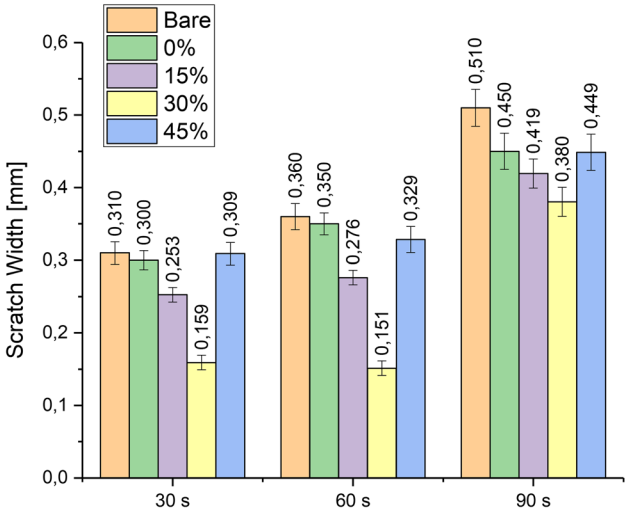

Fig. 16 Results and comparison of scratch test in terms of the width of the tracks [mm]

4. Conclusions

- The first result obtained after the study conducted is represented by the possibility of making coatings with each of the mixtures of powders used (pure aluminum, 15% Al_2O_3, 30% Al_2O_3, and 45% Al_2O_3); therefore, the cold spray system seems to be an effective method to create composite metallic coatings on hemp-PLA composite substrates. Moreover, according to SEM analysis, a good (but can be further improved) compaction of the coating is obtained.
- Alumina particles are not able to form a coating on their own, but they cause a roughening of the impacted surface and carry out a peening effect of it. This causes an increase in the adhesion of the subsequent layers due to the micro-asperities formed.
- As the alumina percentage increases, roughness turns out to be increasing up to 500% in passing from the coating containing 30% Al_2O_3 to that with 45%.
- Introduction of alumina in the mixture leads to an improvement in the surface properties of the components in terms of wear behavior, up to the 60% when the concentration of Al_2O_3 does not exceed the 15%. A further increase of this wt.% to 45% Al_2O_3, causes deterioration of the surface. The scratch behavior has a similar trend to the wear behavior, with the best performances reached with an alumina content of 30%.
- Observing the tribological analyses carried out, it can be said that the best characteristics, in terms of process efficiency and quality of coatings, are obtained with the mixture of powders with 30% Al_2O_3.

Furthermore, the studied process allows to carry out partial coatings of the substrate which can give different properties to a single part of a component.

References

1. P. Carlone, F. Rubino, V. Paradiso, and F. Tucci, Multi-Scale Modeling and Online Monitoring of Resin Flow Through Dual-Scale Textiles in Liquid Composite Molding Processes, *Int. J. Adv. Manuf. Technol.*, 2018, https://doi.org/10.1007/s00170-018-1703-9
2. L.G. Blok, M.L. Longana, H. Yu, and B.K.S. Woods, An Investigation into 3D Printing of Fibre Reinforced Thermoplastic Composites, *Addit. Manuf.*, 2018, **22**, p 176–186. https://doi.org/10.1016/j.addma.2018.04.039
3. X. Wang, M. Jiang, Z. Zhou, J. Gou, and D. Hui, 3D Printing of Polymer Matrix Composites: A Review and Prospective, *Compos. Part B Eng.*, 2017, **110**, p 442–458. https://doi.org/10.1016/j.compositesb.2016.11.034
4. D. Aleksendrić, P. Carlone, and V. Ćirović, Optimization of the Temperature-Time Curve for the Curing Process of Thermoset Matrix Composites, *Appl. Compos. Mater.*, 2016, **23**(5), p 1047–1063. https://doi.org/10.1007/s10443-016-9499-y
5. C. Scarponi, F. Sarasini, J. Tirillò, L. Lampani, T. Valente, and P. Gaudenzi, Low-Velocity Impact Behaviour of Hemp Fibre Reinforced Bio-Based Epoxy Laminates, *Compos. Part B Eng.*, 2016, **91**, p 162–168. https://doi.org/10.1016/j.compositesb.2016.01.048
6. F. Rubino, V. Paradiso, A. Astarita, P. Carlone, and A. Squillace, *Advances in Titanium on Aluminium Alloys Cold Spray Coatings*, 2017, https://doi.org/10.1007/978-3-319-67183-3_7
7. J. Villafuerte, Current and Future Applications of Cold Spray Technology, *Met. Finish.*, 2010, **108**(1), p 37–39. https://doi.org/10.1016/s0026-0576(10)80005-4
8. H. Assadi, H. Kreye, F. Gärtner, and T. Klassen, Cold Spraying—A Materials Perspective, *Acta Mater.*, 2016, **116**, p 382–407. https://doi.org/10.1016/j.actamat.2016.06.034
9. M. Diab, X. Pang, and H. Jahed, The Effect of Pure Aluminum Cold Spray Coating on Corrosion and Corrosion Fatigue of Magnesium (3% Al–1% Zn) Extrusion, *Surf. Coat. Technol.*, 2017, **309**, p 423–435. https://doi.org/10.1016/j.surfcoat.2016.11.014
10. A. Moridi, S.M. Hassani-Gangaraj, and M. Guagliano, On Fatigue Behavior of Cold Spray Coating, *MRS Proc.*, 2014, **1650**, p mrsf13-1650-jj05-03. https://doi.org/10.1557/opl.2014.438
11. V.K. Champagne, The Cold Spray Materials Deposition Process. Fundamental an Aplications, 2007
12. A. Sova, R. Maestracci, M. Jeandin, P. Bertrand, and I. Smurov, Kinetics of Composite Coating Formation Process in Cold Spray: Modelling and Experimental Validation, *Surf. Coat. Technol.*, 2017, **318**, p 309–314. https://doi.org/10.1016/j.surfcoat.2016.06.084
13. A.P. Alkhimov, V.F. Kosarev, and S.V. Klinkov, The Features of Cold Spray Nozzle Design, *J. Therm. Spray Technol.*, 2001, **10**, p 375–381. https://doi.org/10.1361/105996301770349466
14. T. Schmidt, F. Gärtner, H. Assadi, and H. Kreye, Development of a Generalized Parameter Window for Cold Spray Deposition, *Acta Mater.*, 2006, **54**, p 729–742. https://doi.org/10.1016/j.actamat.2005.10.005

15. W.Y. Li, C. Zhang, X.P. Guo, G. Zhang, H.L. Liao, C.J. Li, and C. Coddet, Effect of Standoff Distance on Coating Deposition Characteristics in Cold Spraying, *Mater. Des.*, 2008, **29**, p 297–304. https://doi.org/10.1016/j.matdes.2007.02.005
16. P.C. King, G. Bae, S.H. Zahiri, M. Jahedi, and C. Lee, An Experimental and Finite Element Study of Cold Spray Copper Impact onto Two Aluminum Substrates, *J. Therm. Spray Technol.*, 2010, **19**, p 620–634. https://doi.org/10.1007/s11666-009-9454-7
17. K. Spencer, D.M. Fabijanic, and M.-X. Zhang, The Use of Al–Al2O3 Cold Spray Coatings to Improve the Surface Properties of Magnesium Alloys, *Surf. Coat. Technol.*, 2009, **204**, p 336–344. https://doi.org/10.1016/J.SURFCOAT.2009.07.032
18. B. AL-Mangour, R. Mongrain, E. Irissou, and S. Yue, Improving the Strength and Corrosion Resistance of 316L Stainless Steel for Biomedical Applications Using Cold Spray, *Surf. Coat. Technol.*, 2013, **216**, p 297–307. https://doi.org/10.1016/j.surfcoat.2012.11.061
19. R. Lupoi and W. O'Neill, Deposition of Metallic Coatings on Polymer Surfaces Using Cold Spray, *Surf. Coat. Technol.*, 2010, **1**, p 1. https://doi.org/10.1016/j.surfcoat.2010.08.128
20. D. Giraud, F. Borit, V. Guipont, M. Jeandin, J.M. Malhaire, Metallization of a Polymer Using Cold Spray: Application to Aluminum Coating of Polyamide 66, in *Int. Therm. Spray Conf. Expo. - Air, Land, Water Hum. Body Therm. Spray Sci. Appl. ITSC 2012*. (2012) pp. 265–270
21. F. Rubino, M. Pisaturo, A. Senatore, P. Carlone, and T.S. Sudarshan, Tribological Characterization of SiC and B4C Manufactured by Plasma Pressure Compaction, *J. Mater. Eng. Perform.*, 2017, https://doi.org/10.1007/s11665-017-3016-9
22. A. Moridi, S.M. Hassani-Gangaraj, M. Guagliano, and M. Dao, Cold Spray Coating: Review of Material Systems and Future Perspectives, *Surface Eng.*, 2014, **30**(6), p 369–395. https://doi.org/10.1179/1743294414y.0000000270
23. L. Boccarusso, M. Durante, A. Formisano, A. Langella, F.M.C. Minutolo, Lightweight Bio-composites Based on Hemp Fibres Produced by Conventional and Unconventional Processes, in *AIP Conference Proceedings, 2017*, p. 050015. https://doi.org/10.1063/1.5008060
24. A.D. La Rosa, G. Recca, J. Summerscales, A. Latteri, G. Cozzo, and G. Cicala, Bio-based Versus Traditional Polymer Composites. A Life Cycle Assessment Perspective, *J. Clean. Prod.*, 2014, **74**, p 135–144. https://doi.org/10.1016/j.jclepro.2014.03.017
25. L.T. Drzal, A.K. Mohanty, and M. Misra, Bio-Composite Materials As Alternatives To Petroleum-Based Composites for Automotive Applications, *Magnesium*, 2001, **40**, p 1–3
26. K.N. Bharath and S. Basavarajappa, Applications of Biocomposite Materials Based on Natural Fibers from Renewable Resources: A Review, *Sci. Eng. Compos. Mater.*, 2016, **23**, p 123–133. https://doi.org/10.1515/secm-2014-0088
27. A.N. Netravali and S. Chabba, Composites Get Greener, *Mater. Today*, 2003, **4**(6), p 22–29. https://doi.org/10.1016/s1369-7021(03)00427-9
28. Poly-Lactic Acid Jamshidian, *Production, Applications, Nanocomposites, and Release Studies*, Compr. Rev. Food Sci, Food Saf, 2010
29. E.T.H. Vink, K.R. Rábago, D.A. Glassner, and P.R. Gruber, Applications of Life Cycle Assessment to NatureWorks™ Polylactide (PLA) Production, *Polym. Degrad. Stab.*, 2003, **80**, p 403–419. https://doi.org/10.1016/S0141-3910(02)00372-5
30. A. Le Duigou, P. Davies, and C. Baley, Environmental Impact Analysis of the Production of Flax Fibres to be Used as Composite Material Reinforcement, *J. Biobased Mater. Bioenergy.*, 2011, **5**, p 153–165. https://doi.org/10.1166/jbmb.2011.1116
31. A. Astarita, L. Boccarusso, M. Durante, A. Viscusi, R. Sansone, and L. Carrino, Study of the Production of a Metallic Coating on Natural Fiber Composite Through the Cold Spray Technique, *J. Mater. Eng. Perform.*, 2018, **27**, p 739–750. https://doi.org/10.1007/s11665-018-3147-7
32. A. Shkodkin, A. Kashirin, O. Klyuev, T. Buzdygar, The Basic Principles of DYMET Technology, in: *Int. Therm. Spray Conf.*, 2006, pp. 15–58. https://doi.org/10.1016/b978-0-443-10090-1.50010-4
33. A. Shkodkin, A. Kashirin, O. Klyuev, and T. Buzdygar, Metal Particle Deposition Stimulation by Surface Abrasive Treatment in Gas Dynamic Spraying, *J Them Spray.*, 2006, **1**, p 1. https://doi.org/10.1361/105996306x124383
34. S. Pathak and G. Saha, Development of Sustainable Cold Spray Coatings and 3D Additive Manufacturing Components for Repair/Manufacturing Applications: A Critical Review, *Coatings.*, 2017, **7**, p 122. https://doi.org/10.3390/coatings7080122
35. F. Rubino, P. Carlone, D. Aleksendrić, V. Čirović, L. Sorrentino, C. Bellini, Hard and Soft Computing Models of Composite Curing Process Looking Toward Monitoring and Control, in *AIP Conf. Proc.*, 2016. https://doi.org/10.1063/1.4963438
36. M.-P. Ho, H. Wang, J.-H. Lee, C.-K. Ho, K.-T. Lau, J. Leng, and D. Hui, Critical Factors on Manufacturing Processes of Natural Fibre Composites, *Compos. Part B*, 2012, **43**, p 3549–3562. https://doi.org/10.1016/j.compositesb.2011.10.001
37. L. Boccarusso, L. Carrino, M. Durante, A. Formisano, A. Langella, and F. Memola Capece Minutolo, Hemp Fabric/Epoxy Composites Manufactured by Infusion Process: Improvement of Fire Properties Promoted by Ammonium Polyphosphate, *Compos. Part B Eng.*, 2016, **89**, p 117–126. https://doi.org/10.1016/j.compositesb.2015.10.045
38. M.M. Kabir, H. Wang, K.T. Lau, and F. Cardona, Tensile Properties of Chemically Treated Hemp Fibres as Reinforcement for Composites, *Compos. Part B*, 2013, **53**, p 362–368. https://doi.org/10.1016/j.compositesb.2013.05.048
39. F. Tucci, F. Rubino, P. Carlone, Strain and Temperature Measurement in Pultrusion Processes by Fiber Bragg Grating Sensors, in *AIP Conf. Proc.*, 2018. https://doi.org/10.1063/1.5034837
40. H. Che, P. Vo, and S. Yue, Metallization of Carbon Fibre Reinforced Polymers by Cold Spray, *Surf. Coat. Technol.*, 2017, **313**, p 236–247. https://doi.org/10.1016/j.surfcoat.2017.01.083
41. A. Viscusi, P. Ammendola, A. Astarita, F. Raganati, F. Scherillo, A. Squillace, R. Chirone, and L. Carrino, Aluminum Foam Made via a New Method Based on Cold Gas Dynamic Sprayed Powders Mixed Through Sound Assisted Fluidization Technique, *J. Mater. Process. Technol.*, 2016, **231**, p 265–276. https://doi.org/10.1016/j.jmatprotec.2015.12.030
42. X.L. Zhou, A.F. Chen, J.C. Liu, X.K. Wu, and J.S. Zhang, Preparation of Metallic Coatings on Polymer Matrix Composites by Cold Spray, *Surf. Coat. Technol.*, 2011, **206**, p 132–136. https://doi.org/10.1016/j.surfcoat.2011.07.005
43. A. Ganesan, J. Affi, M. Yamada, and M. Fukumoto, Bonding Behavior Studies of Cold Sprayed Copper Coating on the PVC Polymer Substrate, *Surf. Coat. Technol.*, 2012, **207**, p 262–269. https://doi.org/10.1016/j.surfcoat.2012.06.086
44. D. Rasselet, A. Ruellan, A. Guinault, C. Sollogoub, B. Fayolle, D. Rasselet, A. Ruellan, A. Guinault, G. Miquelard-garnier, Oxidative Degradation of Polylactide (PLA) and Its Effects on Physical and Mechanical Properties, To cite this version: HAL Id: hal-00977105 Science Arts & Métiers (SAM), (2014)
45. R.C. Dykhuizen and M.F. Smith, Gas Dynamic Principles of Cold Spray, *J. Therm. Spray Technol.*, 1998, **7**, p 205–212. https://doi.org/10.1361/105996398770350945
46. S. Kikuchi, Y. Hirota, and J. Komotori, Effect of Specimen Hardness and Shot Particle Hardness on Residual Stress and Fatigue Properties of SCM435H Steel Performed by Fine Particle Peening, *Zair. Soc. Mater. Sci. Japan.*, 2010, **60**, p 547–553. https://doi.org/10.2472/jsms.60.547
47. K.B. Tator, ASM Handbook, Vol 5B: Protective Organic Coatings, (2015)
48. E. Irissou, J.-G. Legoux, B. Arsenault, and C. Moreau, Investigation of Al-Al_2O_3 Cold Spray Coating Formation and Properties, *J. Therm. Spray Technol.*, 2007, **16**, p 661–668. https://doi.org/10.1007/s11666-007-9086-8